Water Cycle 5 (2024) 86–98

Contents lists available at ScienceDirect

Water Cycle

journal homepage: www.keaipublishing.com/en/journals/water-cycle/

Harnessing graphene oxide-enhanced composite metal-organic frameworks for efficient wastewater treatment

Timoth Mkilima [a,*], Yerkebulan Zharkenov [b], Laura Utepbergenova [b], Aisulu Abduova [c], Nursulu Sarypbekova [b], Elmira Smagulova [b], Gulnara Abdukalikova [b], Fazylov Kamidulla [b], Iliyas Zhumadilov [d]

[a] Department of Environmental Engineering and Management, The University of Dodoma, P. O. Box 259, Dodoma, Tanzania
[b] L.N. Gumilyov Eurasian National University, Department of Civil Engineering, Kazakhstan
[c] Ecology" Department. M. Auezov South Kazakhstan Research University, Kazakhstan
[d] Shakarim University, Department of Geodesy and Civil Engineering, Semey City, Kazakhstan

ARTICLE INFO

Keywords:
Carwash wastewater treatment
ZIF-67
ZIF-8
Polyethersulfone
Graphene oxide
Fixed-bed system

ABSTRACT

The issue of carwash wastewater emerges as a pressing environmental concern on a global scale, primarily due to the intricate nature of its pollutants, which makes effective treatment a formidable challenge. In the face of this complex scenario, the pursuit of an efficient treatment methodology assumes paramount importance. In response to this complex scenario, this study embarked on an exploration of a novel polymeric adsorbent material synthesized from Zeolitic Imidazolate Framework-67, Zeolitic Imidazolate Framework-8, Polyethersulfone, and graphene oxide in a fixed-bed treatment system for carwash wastewater. The investigation encompassed three distinct filter column depths, measuring 8 cm, 12 cm, and 16 cm, respectively. With an increase in filter depth from 8 cm to 16 cm, notable improvements were observed in the removal efficiencies for most contaminants. Notably, oils/grease removal showed an increasing trend with column depth, reaching 95.4%, 98.6%, and 100% for 8 cm, 12 cm, and 16 cm depths, respectively. TSS and Turbidity removal efficiencies remained consistently high at 100% across all depths, showcasing effective removal of solid particulate matter. Copper and Zinc removal efficiencies increased with deeper column depths, reaching values of 80.4%–89.9% and 79.6%–90.3%, respectively. Surfactants exhibited efficient removal, with values ranging from 90.6% to 96.6%. Total Dissolved Solids removal efficiency increased from 71.6% to 83.4% as column depth increased. Similarly, Chemical Oxygen Demand, Biochemical Oxygen Demand, total organic carbon, and phosphates removal efficiencies showed improvement with increasing column depth, reaching values of 95.4%, 98.3%, 98.8%, and 89.3%, respectively. Moreover, The composite MOF beads demonstrated significant adsorption capacities in carwash wastewater treatment, with a noteworthy 35.08 mg/g for Oils/Grease and 28.12 mg/g for Biochemical Oxygen Demand, highlighting their efficiency in removing hydrophobic contaminants and organic pollutants.The derived results highlight the potential of the composite material for carwash wastewater treatment towards advancing the field of wastewater treatment.

1. Introduction

Carwash wastewater has become a pressing global environmental concern, driven by its potential to contribute to water pollution and ecological harm. A primary concern comes as a result of the presence of hydrocarbons, oils, and grease within carwash effluents [1]. These contaminants, stemming from vehicle engines and parts, can lead to water body contamination when not handled correctly [2]. Particularly, hydrocarbons are known for their toxicity to aquatic life and their capacity to disrupt the intricate balance of aquatic ecosystems [3]. Moreover, carwash wastewater frequently carries heavy metals such as copper (Cu) and zinc (Zn) originating from brake pads and vehicle surfaces [4]. When released into water bodies, these metals can accumulate in sediments and pose threats to aquatic organisms. Moreover, the detergents and surfactants utilized in carwash operations contain phosphates, which can trigger eutrophication and algal blooms in

* Corresponding author.
E-mail address: tmkilima@gmail.com (T. Mkilima).

https://doi.org/10.1016/j.watcyc.2024.02.005
Received 20 September 2023; Received in revised form 21 February 2024; Accepted 22 February 2024
Available online 28 February 2024

receiving waters, impacting water quality and biodiversity [5]. The combined effect of these contaminants emphasizes the worldwide apprehension linked to the untreated discharge of carwash wastewater into the environment. Another substantial challenge lies in the considerable variability in carwash wastewater composition, influenced by factors such as the vehicle types washed, cleaning products employed, and local regulations. This diversity can complicate treatment endeavors, necessitating tailored approaches to address specific wastewater characteristics [6]. Furthermore, with the ongoing global urbanization and the escalating number of vehicles on the roads, the volume of carwash wastewater generated continues to surge. Without proper treatment and management, this upsurge in wastewater discharge could further strain local water resources and exacerbate pollution issues. To mitigate these concerns, there is a growing need for improved wastewater management practices, including the adoption of eco-friendly cleaning products, the implementation of efficient treatment technologies, and adherence to stringent regulatory standards. Addressing these issues is essential to protect water quality, aquatic ecosystems, and public health on a global scale [7].

To date, diverse physical, chemical, and biological techniques have been harnessed for the treatment of carwash wastewater. Nonetheless, it's worth noting that the realm of carwash wastewater treatment has not received the degree of attention it truly merits within the broader wastewater treatment domain. Among the most prevalent methodologies for carwash wastewater treatment are coagulation [8–10], filtration [2,11,12], adsorption [13], as well as integrated systems [14]. While each of these methods offers valuable utility, they do come with certain design limitations, and exhibit variable treatment performance, effectiveness, and cost implications. Amid this landscape, considerable research efforts have been directed toward the utilization of adsorption processes for general wastewater treatment. This burgeoning body of work underscores the attractiveness of adsorption techniques due to their notable performance, straightforward operational protocols, and economic viability. Furthermore, in recent years, the spotlight has increasingly turned toward the applicability of metal-organic frameworks (MOFs) for wastewater treatment. These MOFs have gained substantial recognition and interest for their exceptional attributes, primarily their superlative surface area. Intriguingly, while MOFs have made significant strides in addressing various environmental challenges, it is surprising that the treatment of carwash wastewater remains an underexplored domain in the MOF applications landscape. However, the broader appeal of MOFs in wastewater treatment arises from several compelling factors, including their tunable and versatile structures, high adsorption capacity, and their potential to address water quality issues in a sustainable and efficient manner. As the world grapples with escalating water resource concerns, MOFs hold promise as a novel and promising avenue for advancing the treatment of carwash wastewater, underscoring their relevance in the evolving landscape of water purification technologies. A significant portion of the existing literature relating to MOFs and wastewater treatment primarily consists of review articles. For instance, Liu et al. [15], conducted a review that explored the utilization of metal-organic frameworks in wastewater treatment. In their research, the authors shed light on the remarkable significance of Metal-Organic Frameworks (MOFs), which consist of metal ions and versatile organic ligands. MOFs have emerged as a leading material due to their exceptional attributes, notably a customizable and precisely defined pore structure. Salehipour et al. [16] conducted an insightful review focusing on the nanoarchitecture of enzyme/MOF composites within the context of wastewater treatment. Their study accentuated that MOFs offer unique advantages as support materials for enzyme immobilization, owing to their remarkable characteristics, such as a porous framework, a high surface area-to-volume ratio, chemical robustness, and the ability to tailor pore sizes. Russo et al.'s [17] comprehensive assessment of the use of MOFs in wastewater treatment focused particularly on adsorption and photodegradation methods. They emphasized that the methods of water purification known as adsorption and photodegradation are two that are incredibly sustainable. These systems have many advantages for treating wastewater, including affordability, simplicity of design, and user-friendliness. Within this framework, MOFs stand out as a ground-breaking class of porous materials distinguished by their crystalline structure. Due to their adjustable qualities and programmable features, MOFs are seen as very attractive candidates for use in wastewater treatment procedures. In the work by Kaur et al. [18], which investigated MOF-based materials for wastewater treatment, the effectiveness of the materials for the removal of hazardous contaminants was the main area of investigation. The study emphasized that a number of pollutants, including organic dyes, antibiotics, heavy metals, pharmaceuticals, and agricultural contaminants, have drawn attention recently within the water industry due to the inadequacy of their removal during traditional water and wastewater treatment processes. MOFs have shown promise as potential solutions to various wastewater management issues.

Zeolitic Imidazolate Framework-8 (ZIF-8) [19] and Zeolitic Imidazolate Framework-67 (ZIF-67) [20] represent two distinct members within the Zeolitic Imidazolate Frameworks (ZIFs) family, a notable subset of metal-organic frameworks (MOFs). These crystalline ZIF materials are prized for their exceptional porosity and distinctive qualities, making them invaluable in a variety of applications. These applications encompass gas storage [21], separation [22], catalysis [23], and adsorption processes [24]. Researchers are actively exploring these materials across a wide spectrum of environmental and industrial contexts, ranging from the purification of water and gases by removing pollutants to the advancement of sophisticated catalytic systems [25–27].

Moreover, within the realm of materials science, a prevailing observation underscores the conventional synthesis of Metal-organic frameworks (MOFs) in powder form, a limitation that proves to be regrettable when confronted with practical applications like adsorption separation. In response to this challenge and with a profound commitment to advancing MOF particle recycling, a novel strategy emerges – the amalgamation of these materials into composite structures alongside polymers like polyether sulfone (PES) [28]. While a myriad of techniques, including the intricate high internal phase emulsions (HIPEs), have been explored for the generation of nanocomposite beads adorned with spherical contours, they often grapple with formidable impediments, including the necessity for high-temperature coatings and convoluted, time-intensive procedures. In this dynamic landscape, the application of the phase inversion approach becomes significant, characterized by its celerity and simplicity, showcasing remarkable prowess in crafting adsorbent beads through the harmonious synergy of polymers and MOFs. Emphasizing the real-world implications, where industrial applications predominantly unfold within continuous systems, the pursuit of knowledge within the realm of fixed bed adsorption assumes paramount significance, bearing the potential for future scalability [29]. On the other hand, graphene oxide (GO) holds immense potential for integration with Polyethersulfone (PES), Zeolitic Imidazolate Framework-8 (ZIF-8), and Zeolitic Imidazolate Framework-67 (ZIF-67) due to its remarkable properties. Graphene oxide (GO), derived from graphene, possesses a unique two-dimensional structure characterized by a substantial surface area, impressive mechanical strength, and exceptional electrical conductivity. These inherent qualities position GO as an invaluable candidate for enhancing the properties of composite materials. When integrated into the composite with ZIF-67 and ZIF-8, GO contributes to improved mechanical reinforcement, heightened thermal stability, and enhanced electrical conductivity. Beyond these benefits, GO's functional groups and expansive surface area open doors for precise chemical modifications and efficient adsorption capabilities. These features collectively endow GO with versatility, making it a pivotal component for tailoring the composite's performance across various applications, including filtration, catalysis, and sensing [30]. As a result, GO's compatibility with PES, ZIF-8, and ZIF-67 fosters a synergistic approach to crafting advanced composite

materials endowed with a wide array of desirable properties and the potential for diverse applications.

The study undertook an examination of an innovative polymeric adsorbent material resulting from the synthesis of Polyethersulfone, Zeolitic Imidazolate Framework-8, and Zeolitic Imidazolate Framework-67. To unleash its capabilities, the study encompassed the exploration of three discrete filter column depths, specifically measuring 8 cm, 12 cm, and 16 cm, respectively.

2. Materials and methods

2.1. Adsorbent material preparation

In the synthesis process, polymeric composite beads were meticulously crafted using a precise phase inversion technique. The procedure involved the preparation of a polymeric solution with precision. Specifically, a mixture of 1.5 g of Polyethersulfone (PES) and 0.5 g of Polyvinylpyrrolidone (PVP) in 5.5 g of N,N-Dimethylacetamide (DMAc) solvent was carefully blended at a controlled room temperature of 25°C for 24 hours to ensure optimal polymer dissolution and homogeneity. Additionally, 1.5 g of Zeolitic Imidazolate Framework-8 (ZIF-8) and Zeolitic Imidazolate Framework-67 (ZIF-67) materials were dispersed with precision. The polymeric solution was then introduced into pure water using an automated pump, ensuring accurate drop-by-drop dispensing. This controlled approach guaranteed the flawless formation of the composite beads, providing unequivocal confirmation of the successful completion of the phase inversion process.

These composite beads underwent a planned controlled drying procedure after synthesis in order to enhance their characteristics. The drying process was carried out in a well-regulated environment that was kept at a constant temperature of 40 ^{0}C. The glass transition temperature of the polymer and the thermal stability of MOF components were taken into account while choosing this temperature to ensure no degradation took place. The drying procedure lasted exactly 12 hours, promoting uniform drying and reducing the likelihood of flaws. Scanning electron microscopy (SEM) was used to characterize the synthetic composite beads. The dependability of the data was increased by using this characterization method to provide a full grasp of the bead structure and composition.

GO was uniformly dispersed in deionized water using a sonication technique that took approximately 4 h and used a sonication power of 150 W as part of the GO dispersion preparation. This careful method produced a stable and evenly disseminated GO solution, which was essential for successfully incorporating GO into the composite. The PES-ZIF-8-ZIF-67 combination was gradually infused with the GO dispersion while being blended with it, all the while maintaining constant stirring at a controlled pace of 300 RPM. According to the desired characteristics for the composite beads, the amount of GO added was precisely regulated to produce a concentration of 5% (w/w) in comparison to the other components. Also, the composite material's homogeneity was done in a methodical manner. For an additional 2 h, mechanical stirring was used to ensure uniform dispersion. After that, a high-frequency probe sonicator operating at 40 kHz was used for 30 min of ultrasonication. Then, a high-speed homogenizer was used to do high-shear mixing for 15 min at 10,000 RPM. These precise processing procedures were essential in ensuring that GO was seamlessly incorporated with the other composite parts, producing a properly blended and homogenous substance.

The Brunauer-Emmett-Teller (BET) data was obtained through nitrogen adsorption-desorption experiments conducted using an ASAP 2020 Physisorption Analyzer. Prior to analysis, ZIF-8, ZIF-67, and the composite material were synthesized following established procedures. The samples were degassed under vacuum to remove any adsorbed impurities. Nitrogen adsorption isotherms were measured at 77 K, covering a wide range of relative pressures. The BET equation was applied to the adsorption data, and the resulting plots allowed for the determination of specific surface areas, pore volumes, and pore size distributions. Micropore, mesopore, and macropore contributions were discerned based on the shape of the isotherms and the corresponding hysteresis loops. This rigorous experimental approach provided precise BET data, enabling a detailed assessment of the materials' surface characteristics and porosity, forming a foundation for the subsequent discussions on their adsorption capabilities and material properties in the Results and Discussion section.

2.2. Experimental setup

The continuous flow adsorption experiment was conducted in a well-constructed Pyrex cylindrical column. With an inner diameter of 1.2 ercentimeters and three various heights, this column had three distinct column depths: adsorbent material that was 10 cm, 15 cm, and 20 cm deep. The created adsorbent material, each measuring 2 mm in size, was poured into the filter depth to obtain the necessary bed height. To ensure the integrity of the adsorbent beads and prevent them from being washed away during the experimentation, a layer of 1-mm glass beads was ingeniously employed to provide support for both ends. The flow rate across all experimental setups was consistently set at 2 mL per minute, maintaining precision and uniformity throughout. Remarkably, the pre-treatment of colored wastewater was executed through an adsorption process carried out within an ultrasonic apparatus. Subsequently, this treated wastewater was continuously introduced into the column, utilizing an upward flow configuration driven by a precise peristaltic pump. At various time intervals, samples were meticulously collected from the effluent location of the column. These samples were then subjected to thorough analysis, employing appropriate and sophisticated analytical techniques to precisely measure and evaluate their concentrations. The overarching concept and setup of this continuous adsorption process are eloquently depicted in Fig. 1, providing an insightful visual representation of the experimentation.

2.3. The employed analytical methods

Wastewater samples were acquired using 5-liter plastic containers that were thoroughly cleaned with deionized water before use. Each collected sample was stored at a constant temperature of 4°C until it underwent detailed analytical testing. In the investigation of system performance, eleven water quality parameters, including Hydrocarbons

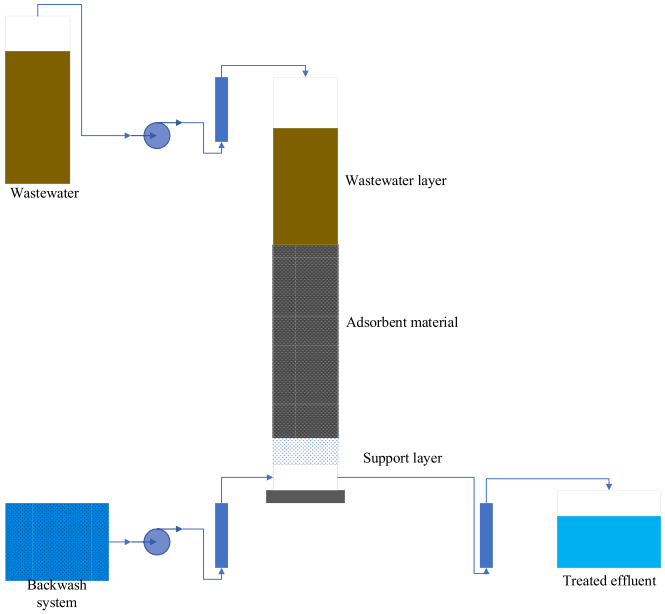

Fig. 1. General treatment setup.

(Oils/Grease), total suspended solids (TSS), Cu, Zn, Detergents (Surfactants), Turbidity, Total Dissolved Solids (TDS), Chemical Oxygen Demand (COD) and Biochemical Oxygen Demand (BOD), total organic carbons (TOC), and phosphates, were examined. The assessment of Hydrocarbons (Oils/Grease) involved the use of the Gravimetric Analysis method, which entailed extracting a known volume of the water sample with a suitable organic solvent, such as n-hexane or petroleum ether. After that, the recovered hydrocarbons were separated from the organic phase and taken out of the aqueous phase. A thorough solvent evaporation method was then used to validate the presence of hydrocarbon residues. These residues were weighed precisely, which made it possible to calculate the hydrocarbon concentration—which is normally represented in milligrams per liter (mg/L) units—exactly. The determination of total suspended solids followed the Standard Method 2540D. Initially, a water sample was filtered through pre-weighed filter paper, capturing the suspended particulates. The filter paper, containing the retained solids, was then carefully dried to remove any residual moisture. The increase in weight of the filter paper after drying provided an accurate measure of the suspended particle content in the sample, which was expressed in milligrams per liter (mg/L). For the estimation of copper (Cu) and zinc (Zn) concentrations, the Inductively Coupled Plasma-Optical Emission Spectrometry (ICP-OES) technology was employed. This precise analytical technique allowed for the accurate quantification of the metal concentrations. The resulting values, also reported in milligrams per liter (mg/L), were obtained after the digestion process, which ensured proper degradation of organic substances in the water samples. To determine detergent (surfactant) concentrations, the Methylene Blue Active Substances (MBAS) Method was utilized. In this method, the water sample was mixed with the MBAS reagent, resulting in the formation of a distinctive blue complex with surfactants. Through meticulous calculations and spectrophotometric measurements at a specific wavelength, the detergent concentrations were determined and reported in milligrams per liter (mg/L). Turbidity measurements were carried out using the Nephelometric Method (ISO 7027). This method allowed for the assessment of the scattering of light caused by suspended particles in the water, providing a quantitative measure of turbidity. This required passing light through the water sample at a 90-degree angle using a nephelometer. Nephelometric turbidity units (NTU), an exact measurement of water purity, were used to express the measured scattered light. The Gravimetric Evaporation technique was used to assess TDS. The water sample must first evaporate to a certain extent before the remaining dissolved particles can be measured using this type of examination. Parts per million (ppm) or milligrams per liter (mg/L) were used to present the statistics.

The concentrations of COD (Chemical Oxygen Demand) and BOD (Biochemical Oxygen Demand) were determined using the Standard Methods 5220 for BOD and 5220D for COD. These procedures required the quantification of the amount of oxygen consumed during chemical oxidation (for COD) or microbial decomposition of organic compounds (for BOD). The samples were incubated for specified periods, and changes in dissolved oxygen or chemical oxygen demand were observed during this time. To measure the Total Organic Carbon (TOC), either the UV-Persulfate Oxidation method or the High-Temperature Combustion method was employed. The conversion of organic carbon into carbon dioxide was measured to calculate the TOC. The results were reported in milligrams per liter (mg/L) or parts per million (ppm). For the assessment of phosphate concentrations, the Standard Method 4500-P was used. In this process, acid digestion transformed phosphate ions into orthophosphate. These ions then reacted with ammonium molybdate and potassium antimony tartrate to form a blue complex. Through spectrophotometric analysis, the phosphate concentrations were estimated and expressed in milligrams per liter (mg/L).

2.4. Modelling of break-through curves

The study also involved an examination of breakthrough curves using two mathematical models, namely the Adams-Bohart model, Yoon and Nelson, Yan and Clark. The investigation of breakthrough curves within the context of fixed-bed adsorption columns holds significant importance due to its multifaceted implications. These curves function as a critical diagnostic tool, facilitating the assessment of system performance, the fine-tuning of operational parameters, and the anticipation of real-world applicability. By pinpointing the point at which adsorbent materials become saturated, breakthrough curves offer insights into process efficiency and guide adjustments to enhance pollutant removal. They play a pivotal role in transitioning from laboratory-scale experiments to industrial implementations, ensuring alignment with environmental regulations. Moreover, studying breakthrough curves is essential for improving our comprehension of adsorption kinetics, which in turn helps us manage processes and find solutions to associated problems. Simply put, breakthrough curve analysis is essential for assuring the effectiveness and efficiency of wastewater treatment and the successful removal of pollutants inside fixed-bed adsorption systems.

The Adams-Bohart model is a frequently used mathematical framework in the study of adsorption. It is a useful tool for clarifying how solute molecules behave as they move through the adsorption column. Researchers can determine important parameters like adsorption capacity and rate of adsorption through the analysis of experimental breakthrough data and its alignment with this model, providing invaluable insights for the optimization of adsorption processes and the design of effective water treatment systems. Equation (1) provides a succinct summary of this paradigm.

$$\frac{C_e}{C_0} = \exp\left(-\frac{K}{Q} \times V \times t\right) \tag{1}$$

Within the Adams-Bohart model equation, the symbol C_e holds significance, representing the concentration of the solute in the effluent. This concentration reflects the presence of the solute within the fluid that exits the adsorption column, typically measured in units such as mg/L or ppm. C_0 represents the initial solute concentration in the influent, which is the fluid entering the column before interacting with the adsorbent, also typically measured in units like mg/L or ppm. K denotes the linear adsorption constant or rate constant, a parameter unique to the adsorption process, characterizing the adsorbent's ability to adsorb the solute. A higher K implies a more robust adsorption capacity, with units depending on those used for Q and V in equation. Q signifies the volumetric flow rate of the influent solution, indicating how quickly the solution passes through the adsorption column, measured in units like L/min or m^3/h. V represents the volume of the adsorption column or bed, typically measured in units like liters (L) or cubic meters (m^3), representing the total volume of the adsorbent material in the column. Lastly, t denotes the contact time, signifying the duration the influent solution interacts with the adsorbent material within the column, usually measured in units like minutes (min) or hours (h).

Yoon and Nelson have introduced a notably straightforward model that stands out for its simplicity compared to alternative models [31]. What sets it apart is its minimal need for intricate data pertaining to the adsorbate's characteristics, the specific adsorbent used, or the physical properties of the adsorption bed. In their equation for a single-component system, they define K_{YN} as the rate constant (expressed in 1/min), τ as the time necessary for 50% adsorbate breakthrough (in minutes), and 't' as the breakthrough time for sampling (in minutes). The Yoon-Nelson equation can be summarized as follows (Equation (2)).

$$\frac{C_e}{C_0} = \frac{1}{1 + e^{K_{YN}(t-1)}} \tag{2}$$

Yan et al. [32] introduced an empirical equation that addresses the limitation of the Thomas model, particularly its significant shortcoming in accurately forecasting the effluent concentration at time zero. In the

Yan model, K_y represents the kinetic rate constant (in L/min/mg), while q_y stands for the maximum adsorption capacity (in mg/g) of the adsorbent as estimated in the Yan model.

$$\frac{C_e}{C_0} = 1 - \frac{1}{1 + \left(\frac{Q^2 t}{K_y q_y m}\right)^{\frac{K_y C_0}{Q}}} \tag{3}$$

The model established by Clark (Equation (4)) relies on the incorporation of mass transfer principles combined with the Freundlich isotherm [33]. Here, the parameters A and r pertain to the kinetic equation, while the exponent n corresponds to the exponent in the Freundlich isotherm.

$$\frac{C_e}{C_0} = \left(\frac{1}{1 + Ae^{-rt}}\right)^{\frac{1}{n-1}} \tag{4}$$

2.5. The applied statistical methods

2.5.1. Analysis of variance

In the context of this study, the adoption of single-factor analysis of variance (ANOVA) was employed as a strategic tool to discern the existence of statistically significant disparities within the intricate matrix of water quality data. It is of paramount importance to accentuate that this methodological approach meticulously evaluates the magnitude of divergence intrinsic to each cluster of water quality data, thoughtfully culled from their individualized cohorts. The evaluation of statistical significance was meticulously executed through a meticulous juxtaposition of the computed p-values against the well-defined alpha threshold, a priori set at 0.05. It merits explicit mention that even in instances where the null hypothesis retains its veracity, the alpha value epitomizes the probability of its prospective repudiation. The veracity of the null hypothesis subsists in cases where the resultant p-value eclipses the stipulated alpha threshold. Speaking to the nuanced role of the p-value, it serves as an exquisite indicator of the likelihood of attaining an outcome more exceptionally divergent from the outcomes of the experimental venture [34,35].

In the conducted study, Scheffé analysis played a pivotal role as a statistical tool for the comprehensive comparison of various treatment scenarios. Following an initial analysis of variance (ANOVA) to assess the significance of differences among multiple groups, Scheffé analysis was employed to conduct rigorous multiple pairwise comparisons among these groups. This method was particularly valuable in determining which specific treatment pairs exhibited statistically significant differences in the study's context. By controlling the familywise error rate and providing conservative yet robust assessments of significance, Scheffé analysis ensured a meticulous examination of the treatment effects, contributing crucial insights into the research findings. Furthermore, the Bonferroni and Holm procedures were employed as crucial statistical methods to effectively manage the issue of multiple comparisons when assessing treatment effects. After conducting an initial analysis of variance (ANOVA) to examine differences among multiple groups, these techniques were utilized to adjust p-values for each pairwise comparison within the study. The Bonferroni correction method, recognized for its conservative approach, was implemented to maintain rigorous control over the familywise error rate, thereby minimizing the risk of Type I errors (false positives). Simultaneously, the Holm procedure was employed, offering a stepwise adjustment of p-values, striking a balance between stringent control and potentially increased analysis power. Through the application of these correction procedures, the study adeptly tackled the challenge of conducting numerous tests, delivering dependable insights into the significance of specific treatment pair differences and bolstering the overall statistical validity of the findings.

2.5.2. Correlation analysis

Moreover, the research aimed to explore potential interrelationships among various water quality parameters, seeking to unveil the extent to which one parameter might serve as a reliable indicator or exert an influence on another. Furthermore, the study delved into the intricate connections between different parameters, particularly their impact on the overall effectiveness of the systems under investigation. The scale indicating the strength of the relationship between variables is as follows: A range of 0–0.29 signifies a low relationship, 0.3 to 0.49 represents a moderate relationship, 0.5 to 0.69 suggests a considerable relationship and a range of 0.7–1 indicates a substantial relationship.

3. Results

3.1. Material characterization

Fig. 2 provides a detailed SEM analysis of the synthesized materials, offering a profound exploration of the structural and surface characteristics of distinct constituents, namely, pure Zeolitic Imidazolate Framework-8 and Zeolitic Imidazolate Framework-67 particles, in addition to the polymeric composite beads. The SEM imaging has unveiled a wealth of intricate insights into the internal and surface properties of these components. Upon meticulous examination of the cross-sectional image of the Polyethersulfone bead, a captivating textural-like pattern emerges, underscoring the presence of clearly discernible macro-pores within the bead's internal structure. Notably, the surface of the Polyethersulfone bead exhibits a strikingly smooth and uniform appearance, devoid of any detectable particles or irregularities. This polished surface signifies the integrity and purity of the Polyethersulfone material. In stark contrast, the SEM images offer a vivid portrayal of a remarkable phenomenon occurring within the polymeric composite beads. Zeolitic Imidazolate Framework-8 and Zeolitic Imidazolate Framework-67 particles are not only conspicuously present but also meticulously dispersed and expertly coated onto the surface of these beads. This fascinating discovery highlights a significant migration of Metal-Organic Framework (MOF) particles from the interior of the composite material to its outer surface. This migration has direct consequences, leading to noticeable alterations on the surface of the polymeric composite. These alterations manifest as the development of prominent raised areas and depressions. These surface irregularities offer valuable insights into the dynamic interaction between the polymeric matrix and the integrated MOF particles, shedding light on the unique structural characteristics of the resulting composite material.

The BET data (Table 1) reveals distinct characteristics among ZIF-8, ZIF-67, and the composite material. ZIF-8 exhibits the highest surface area at 1285 m^2/g, predominantly comprised of micropores, followed by mesopores and a minor proportion of macropores. In comparison, ZIF-67 demonstrates a slightly lower surface area of 955 m^2/g, characterized by micropores, mesopores, and a consistent fraction of macropores. The composite material, comprising both ZIF-8 and ZIF-67, displays an intermediate surface area of 814 m^2/g, with a distribution of micropores, mesopores, and an increased proportion of macropores. The data indicates variations in the pore structure and surface area, suggesting potential differences in adsorption capabilities and material properties among the three samples.

3.2. Raw wastewater characterization

3.2.1. General characterization

Before implementing any treatment measures, a comprehensive analysis of the wastewater samples was conducted to gain a holistic understanding of the water quality (Table 2). The selection of specific parameters for this analysis was thoughtfully chosen based on their prevalence in carwash wastewater, ensuring that they accurately portray its key characteristics. To begin with, the concentration of hydrocarbons, which represents the presence of oils and grease, was

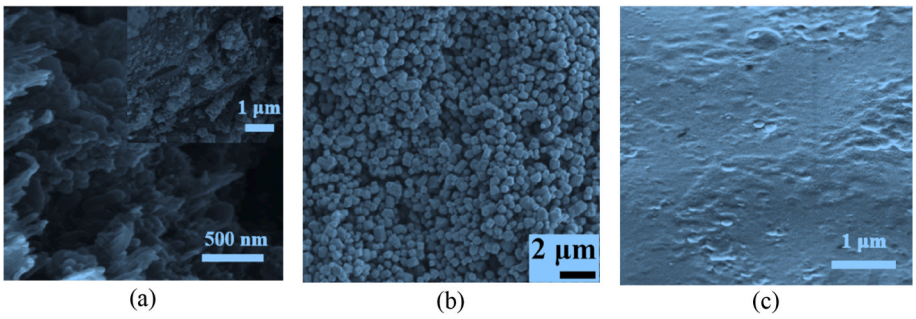

Fig. 2. Morphological characteristics of the material (a) composite material (b) Zeolitic Imidazolate Framework-8 (c) Polyethersulfone.

Table 1
BET data of the investigated MOF.

Parameter	ZIF-8	ZIF-67	Composite
Surface Area (m^2/g)	1285	955	814
Pore Volume (cm^3/g)	0.8	0.6	0.4
Pore Size Distribution	Micropores (<2 nm): 55% Mesopores (2–50 nm): 40% Macropores (>50 nm): 5%	Micropores (<2 nm): 50% Mesopores (2–50 nm): 45% Macropores (>50 nm): 5%	Micropores (<2 nm): 40% Mesopores (2–50 nm): 50% Macropores (>50 nm): 10%

Table 2
Characteristics of the raw wastewater based on the 11 investigated water quality parameters.

Parameter	Min	Max	Mean	Median	STD	Units
Oils/Grease	56.4	98.9	81.56	86.5	14.125	mg/L
TSS	126.9	285.5	201.7	204.7	56.080	mg/L
Copper	4.6	5	4.8	4.8	0.141	mg/L
Zinc	2.34	4.56	3.436	2.96	0.895	mg/L
Surfactants	36.8	44.5	41.2	42.6	2.881	mg/L
Turbidity	80.3	98.5	89.56	89.5	6.033	NTU
TDS	347.8	483.5	413.02	402.7	47.473	mg/L
COD	286.3	492.2	396.64	413.8	68.235	mg/L
BOD	104.4	186.9	145.28	132.2	32.675	mg/L
TOC	34.9	46.6	41.92	42.8	4.199	mg/L
Phosphates	4.6	8.4	6.58	6.9	1.465	mg/L

examined. The findings revealed a concentration range of 56.4 mg/L to 98.9 mg/L, with an average value of 81.56 mg/L. This data underscores a notable presence of hydrocarbon contaminants within the wastewater, signifying its potential as a source of pollution. Similarly, the analysis of suspended solids unveiled concentrations that ranged from 126.9 mg/L to 285.5 mg/L, with an average concentration of 201.7 mg/L. These suspended solids encompass undissolved particles that have the potential to impact water clarity and overall water quality. The assessment of specific heavy metal elements, such as copper and zinc, shows limited fluctuation, with Cu ranging from 4.6 mg/L to 5 mg/L and Zn from 2.34 mg/L to 4.56 mg/L, suggesting a consistent presence of these elements in the sample. Detergent concentrations vary between 36.8 mg/L and 44.5 mg/L, providing insights into the potential presence of cleaning agents or surfactants from various sources. Furthermore, turbidity measurements, within the range of 80.3 NTU to 98.5 NTU, with an average of 89.56 NTU, indicate the potential for haziness or cloudiness in the water due to suspended particles, which is crucial for water quality improvement considerations. TDS range from 347.8 mg/L to 483.5 mg/L, with an average of 413.02 mg/L, offering a comprehensive view of the dissolved content within the water. COD values, spanning from 286.3 mg/L to 492.2 mg/L, with an average of 396.64 mg/L, shed light on the oxygen required for chemical o xidation and indicate the presence of organic pollution. Similarly, BOD values vary from 104.4 mg/L to 186.9 mg/L, with a mean of 145.28 mg/L, reflecting the quantity of oxygen consumed by microorganisms during organic matter decomposition. TOC concentrations ranging from 34.9 mg/L to 46.6 mg/L, with a mean value of 41.92 mg/L, quantify the organic carbon content, contributing to an understanding of potential pollution sources. Lastly, phosphate levels, from 4.6 mg/L to 8.4 mg/L, with an average of 6.58 mg/L, raise concerns due to their impact on aquatic ecosystems and potential contributions to eutrophication. Elevated values in parameters like COD and BOD underscore the presence of a substantial organic load, emphasizing the need for treatment before discharge to protect the environment and public health. The selection of specific treatment processes will depend on local regulatory standards and environmental objectives.

3.2.2. *Correlation analysis*

In the analysis of wastewater samples collected from a car wash, a comprehensive correlation matrix reveals intricate relationships among various parameters (Table 3). Hydrocarbons exhibit a perfect positive correlation with themselves (correlation coefficient of 1), a logical outcome. Suspended solids, on the other hand, show a positive correlation with hydrocarbons (0.3908), implying that as suspended solids concentration increases, there's a modest uptick in hydrocarbons, suggesting a potential association between hydrocarbons and solid particles within the wastewater. Detergents display a strong positive correlation with both hydrocarbons (0.7148) and suspended solids (0.7448), indicating that their concentration closely intertwines with the presence of hydrocarbons and suspended solids in the wastewater, likely owing to the commonplace usage of detergents in car wash runoff. Turbidity exhibits a remarkably strong positive correlation with hydrocarbons (0.9674), implying that as turbidity levels surge, so does the concentration of hydrocarbons. Turbidity often arises from solid particles, hinting at the potential presence of suspended hydrocarbons. TDS demonstrate positive correlations with hydrocarbons (0.6643), suspended solids (0.6650), detergents (0.8942), and turbidity (0.7222), suggesting a shared underlying source or relationship among these variables. COD shows positive correlations with hydrocarbons (0.4499), suspended solids (0.6723), detergents (0.8765), turbidity (0.5394), and TDS (0.5929), underscoring its relevance to various contaminants in the wastewater, as it measures the oxygen needed to chemically oxidize organic and inorganic matter. BOD exhibits positive correlations with all parameters, highlighting a strong relationship with hydrocarbons (0.6545), suspended solids (0.4874), detergents (0.8349), turbidity (0.6603), TDS (0.9760), COD (0.5122), and TOC (0.6367). BOD measurements, which closely resemble a number of other parameters, are essential for determining how much oxygen microbes consume during the breakdown of organic matter. A strikingly strong positive correlation exists between all parameters and TOC, which measures the total concentration of organic carbon compounds. This correlation shows that TOC has a significant relationship with hydrocarbons (0.9690), suspended solids (0.5072), detergents (0.8047), turbidity (0.9691), TDS (0.6576), COD (0.6367), BOD (0.6173), and phosphates (0.6300). This

Table 3
The correlation matrix table from the raw wastewater concentration results.

	Oils/Grease	TSS	Surfactants	Turbidity	TDS	COD	BOD	TOC	Phosphates
Oils/Grease	1								
TSS	0.3908	1							
Surfactants	0.7148	0.7448	1						
Turbidity	0.9674	0.6048	0.7882	1					
TDS	0.6643	0.6650	0.8942	0.7222	1				
COD	0.4499	0.6723	0.8765	0.5394	0.5929	1			
BOD	0.6545	0.4874	0.8349	0.6603	0.9760	0.5122	1		
TOC	0.9690	0.5072	0.8047	0.9691	0.6576	0.6367	0.6173	1	
Phosphates	0.7075	0.7102	0.9479	0.7800	0.7088	0.9472	0.6300	0.8459	1

emphasizes how sensitive TOC is to different pollutants. Last but not least, phosphates show positive correlations with every measure, indicating that they are related to hydrocarbons (0.7075), suspended solids (0.7102), detergents (0.9479), turbidity (0.7800), TDS (0.7088), COD (0.9472), BOD (0.6300), and TOC (0.8459). These results point to a possible relationship between detergents, phosphates, and other pollutants in the wastewater. In summary, this correlation matrix reveals significant and intricate relationships among various parameters within the car wash wastewater samples. These insights are of paramount importance in comprehending the composition and potential sources of contamination within the wastewater, thereby providing essential guidance for designing appropriate treatment processes. However, it is vital to emphasize that correlation does not imply causation and further analyses may be necessary to establish causal relationships or pinpoint specific sources of contamination.

3.3. Removal efficiency

The removal efficiencies of various parameters in carwash wastewater using adsorbent materials at different filter depths reveal several trends (Fig. 3). As the filter depth increases from 8 cm to 16 cm, there is a notable improvement in the removal efficiencies for most contaminants. Hydrocarbons (oils/grease) show a substantial increase in removal efficiency, from 95.4% at 8 cm to 100% at 16 cm, indicating that deeper filtration significantly enhances the removal of these contaminants. Total suspended solids, copper, zinc, surfactants (detergents), water cloudiness (turbidity), and the concentration of dissolved solids all display substantial enhancements in their removal rates as the filter depth increases, ultimately approaching near-complete removal when the depth reaches 16 cm. This indicates that deeper filtration is conducive to improved capture of particles and the adsorption of contaminants. Similarly, parameters like COD, BOD, TOC, and phosphate levels exhibit noticeable boosts in their removal efficiencies as the filter depth increases, showcasing the effectiveness of the adsorbent materials in reducing both organic and inorganic pollutants. In summary, the results indicate that increasing filter depth improves the overall purification efficiency of carwash wastewater, leading to higher removal rates for a wide range of contaminants, making it an effective strategy for wastewater treatment.

3.4. Adsorption capacity

The adsorption capacity values obtained for various parameters during the treatment of carwash wastewater using composite MOF (Metal-Organic Framework) beads, including ZIF-8 and ZIF-67, offer valuable insights into the effectiveness of this method (Fig. 4). Notably, the adsorption capacity for Oils/Grease stands out at 35.08 mg/g, indicating a substantial removal capability for hydrophobic contaminants present in the wastewater. Similarly, TSS exhibit an adsorption capacity of 26.14 mg/g, highlighting the composite MOF's efficiency in capturing solid particulate matter. Copper and Zinc adsorption capacities of 17.96 mg/g and 14.2 mg/g, respectively, suggest successful heavy metal removal. Surfactants, represented by Detergents, display a notable adsorption capacity of 24.48 mg/g, indicating efficient removal of these organic compounds. Turbidity reduction is apparent with an adsorption capacity of 19.12 mg/g, confirming the removal of fine particulate matter. Total Dissolved Solids (TDS) show impressive adsorption capacity at 38.88 mg/g, signifying effective removal of dissolved substances. Moreover, the high adsorption capacities of 48.12 mg/g for Chemical Oxygen Demand (COD), 28.12 mg/g for Biochemical Oxygen Demand (BOD), 33.54 mg/g for Total Organic Carbon (TOC), and 13.92 mg/g for Phosphates underline the composite MOF beads' proficiency in removing organic pollutants and nutrients. In summary, these results collectively demonstrate the versatility and effectiveness of composite MOF beads in treating carwash wastewater, making them a promising candidate for wastewater remediation applications.

A significant factor to consider when designing an adsorption-based water treatment system is the breakthrough point. In this study, Cu,

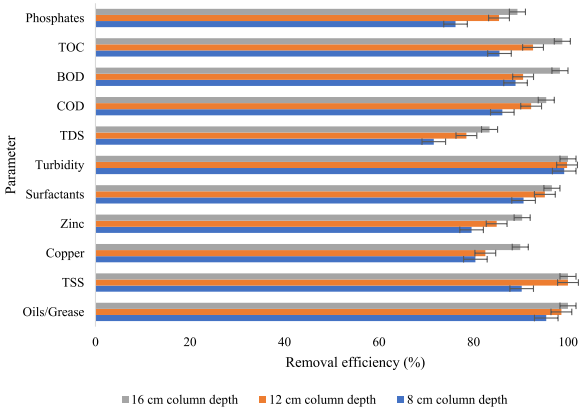

Fig. 3. Removal efficiencies from different parameters.

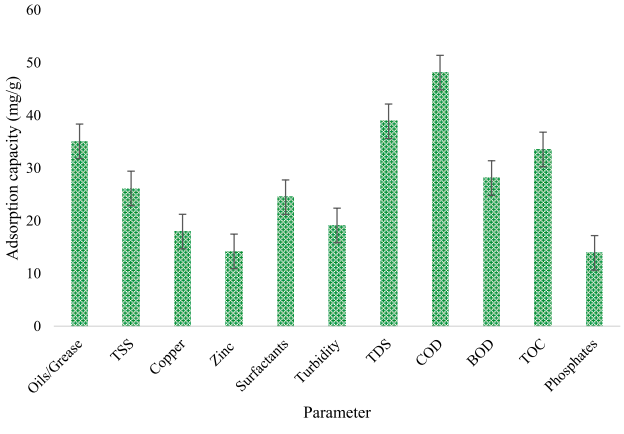

Fig. 4. Adsorption capacities from different parameters.

hydrocarbons (oils/grease), and turbidity were chosen as representative parameters to investigate various aspects of the breakthrough using different non-linear mathematical models. Breakthrough occurs when the filter media becomes saturated with contaminants, and the effluent water quality deteriorates as a result. Designing a fixed-bed filter with an understanding of breakthrough is crucial to ensure that the filter effectively removes contaminants without compromising the treated water's quality. Factors such as filter media selection, flow rate, filter bed depth, and the type of contaminants being treated all play a role in determining when breakthrough will occur. Proper design and monitoring can help extend the filter's lifespan and maintain consistent water quality throughout its operation.

Fig. 5 illustrates the breakthrough curves derived from the experimental data for copper adsorption, alongside corresponding mathematical models, each employing filters of varying depths (8 cm, 12 cm, and 16 cm). Analyzing Fig. 5a, b, and 5c reveals a noteworthy trend: an increase in the depth of the filter bed has a notable impact on delaying the breakthrough points within the curves. The breakthrough point signifies the juncture at which the effluent concentration of the target substance experiences a substantial increase.

Fig. 6 provides a visual representation of the breakthrough curves generated from the experimental data for turbidity adsorption. These curves are accompanied by corresponding mathematical models, namely Bohart-Adams, Clark, Yan and Yoon, and Nelson, each of which utilizes filters with varying depths (8 cm, 12 cm, and 16 cm). Upon a closer examination of these figures, a significant and consistent trend emerges, similar to what was observed for copper adsorption. It becomes evident that an increase in the depth of the filter bed exerts a notable influence on delaying the breakthrough points within the curves. As

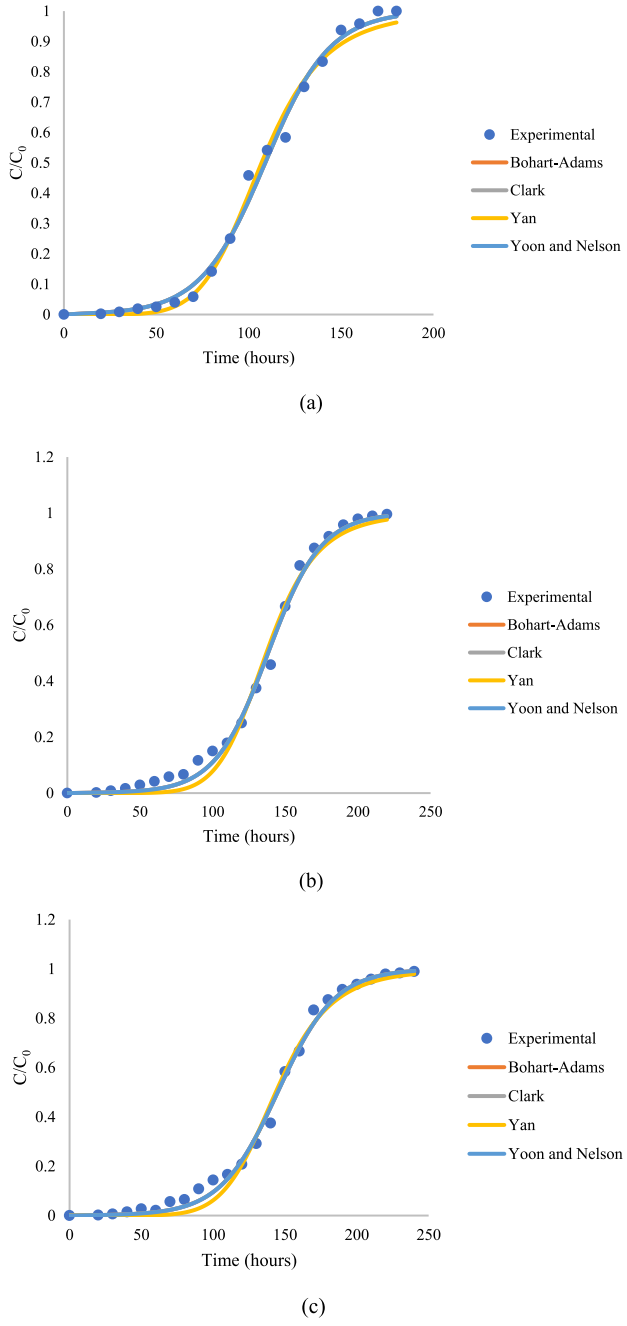

Fig. 5. Breakthrough curves for copper (a) 8 cm column depth (b) 12 cm column depth (c) 16 cm column depth.

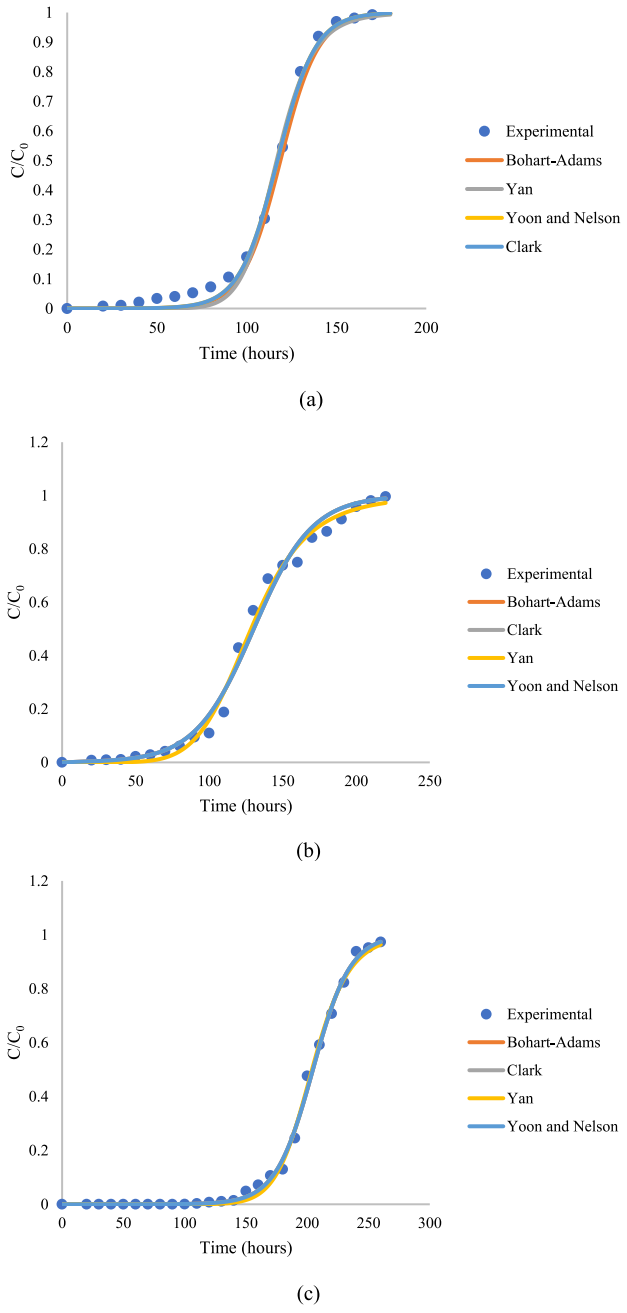

Fig. 6. Breakthrough curves for turbidity (a) 8 cm column depth (b) 12 cm column depth (c) 16 cm column depth.

previously highlighted, the breakthrough point signifies the precise moment at which the effluent concentration of the target substance undergoes a substantial and noticeable increase.

Fig. 7 offers a visual depiction of the breakthrough curves resulting from the experimental data pertaining to the adsorption of hydrocarbons, specifically oils and grease. These curves are presented alongside corresponding mathematical models, including the Bohart-Adams, Clark, Yan and Yoon, and Nelson models, each employing filters with varying depths (8 cm, 12 cm, and 16 cm). Upon closer scrutiny of these graphical representations, a significant and consistent pattern emerges, mirroring the observations made in the context of copper and turbidity adsorption. It becomes increasingly apparent that an augmentation in the depth of the filter bed exerts a substantial influence in prolonging the occurrence of breakthrough points within these curves. This prolonged interaction enhances the effectiveness of the adsorption process, leading to a noticeable postponement of the breakthrough point. In essence, deeper filter beds enhance the filtration system's capability to capture and adsorb hydrocarbons, including oils and grease, thus delaying their appearance in the effluent. This recurring trend underscores the practical significance of selecting an appropriate filter bed depth in designing and optimizing filtration systems, particularly in contexts where efficient removal of hydrocarbons is essential, such as in wastewater treatment and environmental remediation processes.

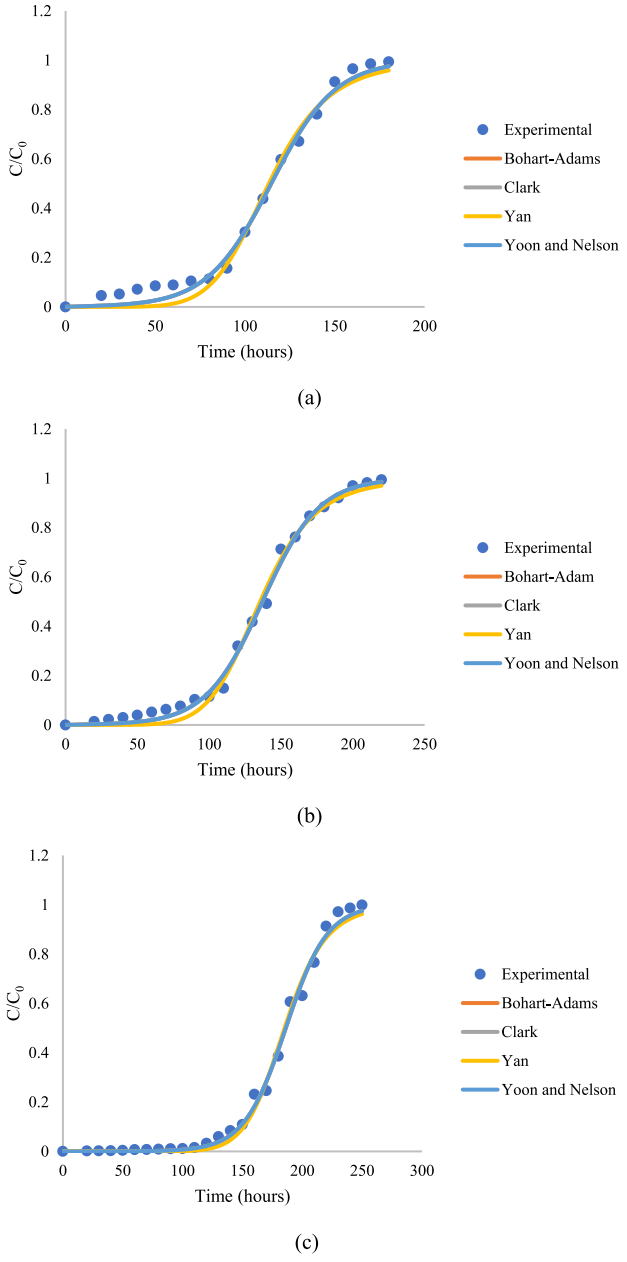

Fig. 7. Breakthrough curves for hydrocarbons (a) 8 cm column depth (b) 12 cm column depth (c) 16 cm column depth.

3.5. Analysis of variance

3.5.1. Based on ANOVA

The analysis of variance (ANOVA) conducted on effluents treated at varying column depths (8 cm, 12 cm, and 16 cm) using a composite MOF (ZIF(67)-ZIF(8)-PES-GO-GO) reveals significant differences in concentration values for various parameters among these column depths (Table 4). These outcomes provide valuable insights into the impact of column depth on the treatment process. Starting with hydrocarbons, the p-value of 3.5873×10^{-13} is markedly smaller than the significance level of 0.05, indicating strong statistical significance. This signifies substantial variations in hydrocarbon concentration (representing oils and grease) across the different column depths. A similar pattern emerges for suspended solids, where the p-value of 1.7999×10^{-20} is significantly less than 0.05, signifying significant differences in suspended solids concentration among the column depths. The analysis extends to heavy metals such as copper and zinc. For copper, the p-value of 8.7097×10^{-10} is well below the significance level, suggesting substantial variations in copper concentration. Likewise, zinc exhibits significant differences in concentration among the column depths, with a p-value of 4.7133×10^{-10}. Detergents, represented by surfactants, also display substantial differences with a p-value of 1.5839×10^{-09}, indicating notable distinctions in detergent concentration among the various column depths. Turbidity, reflecting water cloudiness, exhibits significant variations among the column depths, as evidenced by a p-value of 3.8751×10^{-19}. TDS show significant differences with a p-value of 2.1201×10^{-11}, highlighting variations in dissolved content within the water. COD and BOD, indicators of organic pollution, both exhibit substantial variations among the column depths with low p-values of 1.4367×10^{-16} and 2.7425×10^{-15}, respectively. TOC also displays significant differences with a p-value of 5.8793×10^{-16}. Even phosphates, which can contribute to eutrophication, exhibit notable variations among the column depths with a p-value of 3.2315E-12. Generally, the consistently low p-values across these parameters underscore the significance of column depth (8 cm, 12 cm, or 16 cm) in influencing concentration values in treated effluents. These findings emphasize the importance of considering column depth as a critical factor in the treatment process's efficiency and suggest the need for further investigations or optimization efforts to tailor the treatment process to specific goals and standards effectively.

Table 4
ANOVA results for each of the investigated parameter concentrations in 8 cm filter depth, 12 cm, and 16 cm.

Parameter	p-value	Status (is p-value less than 0.05?)
Oils/Grease	3.5873×10^{-13}	TRUE
Suspended Solids	1.7999×10^{-20}	TRUE
Copper	8.7097×10^{-10}	TRUE
Zinc	4.7133×10^{-10}	TRUE
Detergents (Surfactants)	1.5839×10^{-09}	TRUE
Turbidity	3.8751×10^{-19}	TRUE
Total Dissolved Solids	2.1201×10^{-11}	TRUE
Chemical Oxygen Demand	1.4367×10^{-16}	TRUE
Biochemical Oxygen Demand	2.7425×10^{-15}	TRUE
Total Organic Carbon	5.8793×10^{-16}	TRUE
Phosphates	3.2315×10^{-12}	TRUE

3.5.2. Based on tukey HSD for oils/grease

The results of the Tukey Honestly Significant Difference (HSD) analysis, which examined the removal efficiency of hydrocarbons (oil/grease) among various treatment groups, demonstrate the statistical significance of these differences (Table 5). Specifically, when comparing raw wastewater (RWW) to effluent treated at column depths of 8 cm, 12 cm, and 16 cm (ET-8 cm, ET-12 cm, ET-16 cm), the Q statistic values (22.0889, 22.7865, and 23.0484, respectively) reveal significant disparities in hydrocarbon removal efficiency. Furthermore, the p-values for these comparisons, all registering at 0.001005 (significantly less than the 0.01 significance level), underscore the statistical significance of these observed variations. Conversely, when assessing the differences in hydrocarbon removal efficiency among the treatments with different column depths (ET-8 cm, ET-12 cm, and ET-16 cm), the Q statistic values (0.6977, 0.9596, and 0.2619, respectively) are notably lower. Moreover, the associated p-values for these comparisons are all substantially higher at 0.899995, exceeding the 0.01 significance level, indicating that these differences are not statistically significant (insignificant). In summation, the Tukey HSD analysis reveals a noteworthy discrepancy in hydrocarbon removal efficiency between raw wastewater and effluent treated at various column depths (8 cm, 12 cm, and 16 cm), signifying that deeper filtration enhances hydrocarbon removal. Conversely, no significant differences in hydrocarbon removal efficiency are observed among treatments with different column depths (ET-8 cm, ET-12 cm, and ET-16 cm). This implies that increasing the column depth beyond 8 cm does not substantially augment hydrocarbon removal in this specific study.

3.5.3. Based on scheffé for oils/grease

The Scheffé analysis results provide significant insights into the comparison of different treatment scenarios for wastewater (Table 6). When examining the contrasts between raw wastewater and effluent treated at varying column depths (8 cm, 12 cm, and 16 cm), the Scheffé T-statistics are remarkably high, ranging from 15.6192 to 16.2977, and they are accompanied by extremely low p-values (6.68×10^{-10} to 3.53×10^{-10}), all of which indicate highly significant differences (**$p < 0.01$) between these groups. These findings highlight the substantial impact of different treatment depths on effluent quality, demonstrating that deeper filtration significantly improves purification. Conversely, when comparing different column depths within the treated effluent groups, the Scheffé T-statistics are much lower, and the p-values are notably higher, indicating insignificance. Specifically, the comparisons between 8 cm and 12 cm, 8 cm and 16 cm, and 12 cm and 16 cm column depths all yield insignificant results. These results suggest that once wastewater has undergone treatment, variations in column depths within the treated effluent do not significantly affect the observed parameters.

In the initial combined Bonferroni and Holm table, which includes all possible pairwise comparisons for simultaneous evaluation ($q = 6$), several important findings emerge (Table 7). When comparing raw wastewater to effluent treated at different column depths (8 cm, 12 cm, and 16 cm), all of these comparisons show highly significant results. The

Table 5
Tukey HSD results for each of the investigated parameter concentrations in 8 cm filter depth, 12 cm, and 16 cm.

Treatments pair	Tukey HSD Q statistic	p-value	Tukey HSD inference
RWW vs ET-8 cm	22.0889	0.001005	**$p < 0.01$
RWW vs ET-12 cm	22.7865	0.001005	**$p < 0.01$
RWW vs ET-16 cm	23.0484	0.001005	**$p < 0.01$
ET-8 cm vs ET-12 cm	0.6977	0.899995	insignificant
ET-8 cm vs ET-16 cm	0.9596	0.899995	insignificant
ET-12 cm vs ET-16 cm	0.2619	0.899995	insignificant

Note: RWW = raw wastewater, ET-8 cm = effluent treated by 8 cm column depth, ET-12 cm = effluent treated by 12 cm column depth, ET-16 cm = effluent treated by 16 cm column depth; **$p < 0.01$ = statistically significant.

Table 6
Scheffé results for each of the investigated parameter concentrations in 8 cm filter depth, 12 cm, and 16 cm.

Treatments pair	Scheffé T -statistic	Scheffé p-value	Scheffé inference
RWW vs ET-8 cm	15.6192	6.68×10^{-10}	**$p < 0.01$
RWW vs ET-12 cm	16.1125	4.19×10^{-10}	**$p < 0.01$
RWW vs ET-16 cm	16.2977	3.53×10^{-10}	**$p < 0.01$
ET-8 cm vs ET-12 cm	0.4933	0.969334	insignificant
ET-8 cm vs ET-16 cm	0.6785	0.925928	insignificant
ET-12 cm vs ET-16 cm	0.1852	0.998254	insignificant

Note: RWW = raw wastewater, ET-8 cm = effluent treated by 8 cm column depth, ET-12 cm = effluent treated by 12 cm column depth, ET-16 cm = effluent treated by 16 cm column depth; **$p < 0.01$ = statistically significant.

T-statistics are remarkably high, ranging from 15.6192 to 16.2977, and are accompanied by extremely low p-values, ranging from 1.31×10^{-10} to 2.50×10^{-10}. These findings indicate that there are significant differences between raw wastewater and the treated effluents. These results emphasize the significant impact of different column depths on effluent quality, with deeper filtration leading to significantly improved purification. However, when comparing different column depths within the treated effluent groups, all of these comparisons yield statistically insignificant results. The T-statistics are much lower, and the p-values are notably higher in these cases. This suggests that variations in column depth within the treated effluent do not significantly affect the observed parameters. These findings collectively suggest that the choice of column depth primarily influences the transformation of raw wastewater into treated effluent, with less impact observed within the treated effluent group itself or when compared to the control.

In this subsequent Bonferroni and Holm results, the analysis focused exclusively on a subset of pairwise comparisons that are relevant to treatment raw wastewater (Table 8). This approach is particularly relevant when raw wastewater serves as the control, and the researcher's primary interest is in identifying differences between other treatments and the control. In this specific scenario, there are a total of $q = 3$ relevant pairwise comparisons. The table presents Bonferroni and Holm-adjusted p-values for the observed T-statistic corresponding to these $q = 3$ relevant treatment pairs. These adjusted p-values provide insight into the significance of the differences between raw wastewater and effluent treated at different column depths (8 cm, 12 cm, and 16 cm) relative to treatment raw wastewater (the control). Notably, all three of these pairwise comparisons yield highly significant results, as indicated by the very low p-values (ranging from 4.16×10^{-11} to 1.25×10^{-10}), denoting significant differences (**$p < 0.01$) between raw wastewater and the treated effluents. These findings emphasize that when treatment raw wastewater is used as the control, the differences in effluent quality at various column depths are highly significant, further highlighting the critical role of column depth in the purification process. The color-coded Bonferroni inference in green underscores the significance of these findings, demonstrating that column depth significantly affects the transformation of raw wastewater into treated effluent when compared to treatment raw wastewater (the control).

4. Discussion

The analysis of the raw wastewater revealed crucial insights into its composition and potential environmental consequences. Key findings include the presence of hydrocarbons (oils and grease) at concentrations ranging from 56.4 mg/L to 98.9 mg/L (average: 81.56 mg/L), highlighting its significant pollution potential. It's important to highlight that when hydrocarbons like oils and grease are discharged into aquatic environments, they form a thin layer on the water's surface, which hinders both the exchange of oxygen and the penetration of sunlight [36]. Consequently, this disturbance has adverse effects on aquatic ecosystems, leading to a decrease in dissolved oxygen levels, disruption of photosynthesis, and suffocation of aquatic organisms [37]. Moreover,

Table 7
Results from Bonferroni and Holm tests (comparison of all pairs concurrently) for the tested parameter concentrations at filter depths of 8 cm, 12 cm, and 16 cm.

Treatments pair	Bonferroni and Holm T -statistic	Bonferroni p-value	Bonferroni inference	Holm p-value	Holm inference
RWW vs ET-8 cm	15.6192	2.50×10^{-10}	$^{**}p < 0.01$	1.66×10^{-10}	$^{**}p < 0.01$
RWW vs ET-12 cm	16.1125	1.56×10^{-10}	$^{**}p < 0.01$	$1. 10^{-10}$	$^{**}p < 0.01$
RWW vs ET-16 cm	16.2977	1.31×10^{-10}	$^{**}p < 0.01$	$1. 10^{-10}$	$^{**}p < 0.01$
ET-8 cm vs ET-12 cm	0.4933	3.770845	insignificant	1.256948	insignificant
ET-8 cm vs ET-16 cm	0.6785	3.042773	insignificant	1.521387	insignificant
ET-12 cm vs ET-16 cm	0.1852	5.132428	insignificant	0.855405	insignificant

Note: RWW = raw wastewater, ET-8 cm = effluent treated by 8 cm column depth, ET-12 cm = effluent treated by 12 cm column depth, ET-16 cm = effluent treated by 16 cm column depth; $^{**}p < 0.01$ = statistically significant.

Table 8
Bonferroni and Holm results for each of the examined parameter concentrations in 8 cm, 12 cm, and 16 cm filter depths when only pairs relative to raw wastewater are simultaneously compared.

Treatments pair	Bonferroni and Holm T -statistic	Bonferroni p-value	Bonferroni inference	Holm p-value	Holm inference
RWW vs ET-8 cm	15.6192	1.25×10^{-10}	$^{**}p < 0.01$	4.16×10^{-11}	$^{**}p < 0.01$
RWW vs ET-12 cm	16.1125	7.80×10^{-11}	$^{**}p < 0.01$	5.20×10^{-11}	$^{**}p < 0.01$
RWW vs ET-16 cm	16.2977	6.56×10^{-11}	$^{**}p < 0.01$	6.56×10^{-11}	$^{**}p < 0.01$

Note: RWW = raw wastewater, ET-8 cm = effluent treated by 8 cm column depth, ET-12 cm = effluent treated by 12 cm column depth, ET-16 cm = effluent treated by 16 cm column depth; $^{**}p < 0.01$ = statistically significant.

hydrocarbons have the potential to contaminate both soil and groundwater, which can have a negative impact on plant growth and, in some cases, result in their seepage into water sources, thereby posing a threat to human well-being. Water clarity was affected by the presence of suspended solids, with concentrations ranging from 126.9 mg/L to 285.5 mg/L (average: 201.7 mg/L). Stable concentrations of specific heavy metals, such as Cu and Zn, were observed (Cu: 4.6 mg/L to 5 mg/L, Zn: 2.34 mg/L to 4.56 mg/L). The levels of detergents varied between 36.8 mg/L and 44.5 mg/L, indicating the presence of surfactants. Turbidity, which indicates haziness due to suspended particles, ranged from 80.3 NTU to 98.5 NTU (average: 89.56 NTU). Total dissolved solids (TDS) ranged from 347.8 mg/L to 483.5 mg/L (average: 413.02 mg/L), providing insights into the dissolved content. The values of chemical oxygen demand (COD) varied from 286.3 mg/L to 492.2 mg/L (average: 396.64 mg/L), revealing the extent of organic pollution. Biological oxygen demand (BOD) values fluctuated between 104.4 mg/L and 186.9 mg/L (average: 145.28 mg/L), reflecting the decomposition of organic matter. Total organic carbon (TOC) concentrations ranged from 34.9 mg/L to 46.6 mg/L (average: 41.92 mg/L), quantifying the content of organic carbon. Phosphate levels exhibited variations from 4.6 mg/L to 8.4 mg/L (average: 6.58 mg/L), raising concerns about their impact on aquatic ecosystems. The elevated COD and BOD values underscored a significant organic load, necessitating treatment before discharge to protect the environment and public health. The specific treatment processes should comply with local regulations and align with environmental objectives.

The findings from the study examining the removal efficiencies of various parameters in carwash wastewater using adsorbent materials at different filter depths offer valuable insights into the effectiveness of this purification process. One notable trend observed was a significant improvement in removal efficiencies as the filter depth increased from 8 cm to 16 cm. This improvement was observed across a range of contaminants, including hydrocarbons (oils/grease), suspended solids, heavy metals such as copper (Cu) and zinc (Zn), detergents (surfactants), turbidity, and total dissolved solids (TDS). The achievement of near or complete removal at a 16 cm filter depth highlights the enhanced particle capture and contaminant adsorption capabilities provided by deeper filtration. Deeper filters also demonstrated improved removal efficiencies for organic and inorganic pollutants such as phosphates, chemical oxygen demand (COD), biochemical oxygen demand (BOD), and total organic carbon (TOC). The significant improvement in removal efficiency for parameters like turbidity and total suspended solids (TSS) was particularly noteworthy, reaching up to 100% when a 16 cm filter depth was utilized.

Furthermore, the study revealed important insights into the adsorption capacity of composite MOF beads for removing pollutants from carwash wastewater. The adsorption capability of 35.08 mg/g for oils and grease indicates the composite MOF's potential to efficiently remove hydrophobic contaminants from wastewater. Similarly, the composite MOF exhibited an impressive adsorption capacity of 26.14 mg/g for TSS, highlighting its effectiveness in removing solid particle debris. These findings underscore the potential of composite MOF beads as an effective approach for wastewater treatment.

Based on the adsorption capacities of 17.96 mg/g for copper and 14.2 mg/g for zinc, it was observed that heavy metals were successfully eliminated. The remarkable adsorption capability of detergents, which reached 24.48 mg/g, indicated the effective removal of these organic compounds. Additionally, the reduction in turbidity and an adsorption capacity of 19.12 mg/g provided further evidence of the removal of fine particulate matter. The good adsorption capability of Total Dissolved Solids (TDS) at 38.88 mg/g demonstrated the successful removal of dissolved substances. Furthermore, the high adsorption capacities of 48.12 mg/g for Chemical Oxygen Demand (COD), 28.12 mg/g for Biochemical Oxygen Demand (BOD), 33.54 mg/g for Total Organic Carbon (TOC), and 13.92 mg/g for Phosphates emphasized the effectiveness of composite MOF beads in eliminating organic pollutants and nutrients. In conclusion, these results collectively showcased the versatility and efficiency of composite MOF beads in treating carwash wastewater, making them a promising solution for various wastewater remediation applications. These findings align with those reported in prior studies. For instance, Anifah et al. [38], investigated wastewater oil and grease adsorption using activated carbon derived from sewage sludge. They explored the impact of adsorbent dosage and observed removal efficiencies ranging up to 80% at dosages of 2–4 g/L. The optimal dosage for oil and grease removal was determined to be 4 g/L, with higher dosages leading to increased removal efficiency. Chowdhury et al. [39], conducted a review on the removal of lead ions (Pb^{2+}) from water and wastewater. Their study highlighted that various low-cost adsorbents, including natural materials, industrial byproducts, agricultural waste, forest waste, and biotechnology-based adsorbents, exhibited adsorption capacities within the ranges of 0.8–333.3 mg/g, 2.5–524.0 mg/g, 0.7–2079 mg/g, 0.4–769.2 mg/g, and 7.6–526.0 mg/g, respectively. Furthermore, these adsorbents achieved removal efficiencies of up to 100%.

In the study conducted by et al. [40], research exploring the adsorption capabilities of coconut shell-activated carbon assisted by magnetic particles for eliminating methylene blue dye, it was observed that granular coconut shell-activated carbon (200 Mesh) exhibited a

remarkable 99.7% dye removal efficiency within a mere 2 min. In contrast, the encapsulated activated carbon on regenerated cellulose beads faced challenges in methylene blue uptake, necessitating a longer duration of 90 min for complete adsorption to be achieved.

In the study conducted by Yahya et al. [41], investigation concerning the optimization of a fixed-bed column process for the elimination of Fe (II) and Pb(II) ions from thermal power plant effluent, utilizing NaOH-treated rice husk ash and Spirogyra, significant findings emerged. The study revealed that, when dealing with industrial effluents containing concentrations of 17.9 mg/L and 4.95 mg/L for Fe(II) and Pb(II), respectively, efficient removal rates of 48.29% and 58.30% were achieved. This occurred even in the presence of competing ions and various water quality parameters.

In the study conducted by Kamal et al. [42]; wherby the research focused on continuous flow adsorption for phenol elimination using an eco-friendly, naturally derived bed, noteworthy outcomes were obtained. The activated carbon exhibited its maximum efficiency, removing 86.2% of phenol under conditions of pH 7, an initial phenol concentration of 0.001 M, a bed ratio of 1:3 sand to activated carbon, and a flow rate of 10 ml/min. Additionally, the study delved into the breakthrough behavior of the fixed-bed adsorption process, revealing that the adsorption equilibrium was nearly achieved within 105 min.

In the study conducted by Mouhri et al. [43]; whereby, the research based on continuous adsorption modeling and fixed bed column studies concerning the removal of tannery wastewater pollutants using beach sand. The study observed a correlation between bed height and total adsorption capacity. Specifically, as the bed height increased, the discoloration rates also rose. The 3 cm and 5 cm beds exhibited discoloration rates of 95.4% and 97.4%, respectively, while the maximum fading rate was achieved by the 7 cm bed, nearing 100%. These findings indicate that the height of the bed through which the effluent flows is a significant parameter influencing the performance of continuous adsorption and the column's operation.

From the results of breakthrough curves derived from the experimental data for copper adsorption, oils/grease, and turbidity, it was observed that an increase in the depth of the filter bed has a notable impact on delaying the breakthrough points within the curves [44]. This can be attributed to the fact that deeper beds are observed to provide a longer path for the fluid to travel through, increasing the contact time between the fluid and the adsorbent material [45]. This extended contact time allows for more effective adsorption and often results in a later breakthrough [45]. Expanding upon this observation, it's crucial to grasp the significance of delayed breakthrough points in filtration and adsorption processes. Deeper filter beds offer a lengthier path for fluid flow through the adsorption medium, resulting in increased contact time with the adsorbent material. This prolonged contact enhances the filter's adsorption capacity, allowing it to capture more of the target substance before a breakthrough occurs. In practical terms, deeper filter beds enable the system to treat larger volumes of fluid before the effluent exceeds acceptable concentration limits. This delay in breakthrough is advantageous, as it extends the operational lifespan of the filtration or adsorption system without frequent maintenance or adsorbent replacement. Such insights are invaluable for optimizing filtration processes in applications like wastewater treatment, where delaying breakthrough can enhance efficiency and cost-effectiveness.

5. Conclusion

The study investigated the potential of a novel polymeric adsorbent, synthesized from Zeolitic Imidazolate Framework-67, Zeolitic Imidazolate Framework-8, and Polyethersulfone, for carwash wastewater treatment in a fixed-bed system. The examination of filter column depths (8 cm, 12 cm, and 16 cm) revealed significant improvements in contaminant removal. Deeper filtration proved particularly effective, notably enhancing the removal of hydrocarbons like oils/grease. In addition, other pollutants such as total suspended solids, copper, zinc, surfactants (detergents), turbidity, and dissolved solids showed significant improvements in removal, reaching almost complete elimination with a filter depth of 16 cm. This trend emphasized the effectiveness of deeper filtration in capturing particles and adsorbing contaminants. Moreover, important parameters like COD, BOD, TOC, and phosphates displayed notable increases in removal efficiencies as the filter depth increased, indicating the effectiveness of the adsorbent material in reducing both organic and inorganic pollutants. The composite MOF beads showcased impressive adsorption capacities: Oils/Grease (35.08 mg/g), TSS (26.14 mg/g), Copper (17.96 mg/g), and Surfactants (24.48 mg/g), emphasizing their efficiency in contaminant removal. Notably, turbidity reduction reached 19.12 mg/g, while TDS removal stood at 38.88 mg/g. The investigation into breakthrough curves, particularly for copper adsorption, oils/grease, and turbidity, unveiled a consistent trend. Deeper filter beds exhibited the remarkable ability to delay breakthrough points significantly. This delay was attributed to the extended fluid-path within deeper beds, allowing for more effective adsorption and, consequently, a later breakthrough. This underscores the practical significance of filter bed depth in filtration and adsorption processes, offering valuable insights for system optimization in various applications, especially water treatment. Generally, increasing filter depth substantially improved carwash wastewater treatment efficiency, resulting in higher removal rates for a broad range of contaminants. The outcomes of this study have direct implications for advancing wastewater treatment technologies, offering a sustainable and efficient solution for the carwash industry. Insights gained from the research could be instrumental in shaping future practices, guiding professionals in the field of environmental engineering, and fostering the development of tailored materials for wastewater remediation. This multifaceted approach ensures that the research not only contributes to academic knowledge but also addresses practical challenges in the built environment, aligning with sustainability goals and enhancing the overall impact of the findings.

Funding

This research was funded by the Committee of Science of the Ministry of Science and Higher Education of the Republic of Kazakhstan (Grant No. BR21882415).

CRediT authorship contribution statement

Timoth Mkilima: Writing – review & editing, Writing – original draft, Supervision, Methodology, Investigation, Formal analysis, Conceptualization. **Yerkebulan Zharkenov:** Resources, Investigation, Funding acquisition, Formal analysis. **Laura Utepbergenova:** Resources, Investigation, Data curation. **Aisulu Abduova:** Resources, Formal analysis, Data curation. **Nursulu Sarypbekova:** Resources, Formal analysis, Data curation. **Elmira Smagulova:** Resources, Investigation, Formal analysis, Data curation. **Gulnara Abdukalikova:** Investigation, Formal analysis, Data curation. **Fazylov Kamidulla:** Resources, Investigation. **Iliyas Zhumadilov:** Resources, Investigation.

Declaration of competing interest

The authors declare that they have no known competing financial interests or personal relationships that could have appeared to influence the work reported in this paper.

References

[1] E. Durna, N. Genç, Application of a multiple criteria analysis for the selection of appropriate radical based processes in treatment of car wash wastewater, Environ. Eng. Res. 26 (2020) 200115, https://doi.org/10.4491/eer.2020.115. –0.
[2] C.-Y. Hu, W.-H. Kuan, L.-W. Ke, J.-M. Wu, A study of car wash wastewater treatment by Cyclo-flow filtration, Water 14 (2022) 1476, https://doi.org/10.3390/w14091476.

[3] L.M. Tormoehlen, K.J. Tekulve, K.A. Nañagas, Hydrocarbon toxicity: a review, Clin. Toxicol. 52 (2014) 479–489, https://doi.org/10.3109/15563650.2014.923904.
[4] M.S.S. Bin Ibrahim, N.H. Hashim, Characterization of car wash wastewater from manually dispersed, snow and auto car wash stations, Int. J. Eng. Technol. (2018), https://doi.org/10.14419/ijet.v7i3.23.17257.
[5] W.-H. Kuan, C.-Y. Hu, L.-W. Ke, J.-M. Wu, A review of on-site carwash wastewater treatment, Sustainability 14 (2022) 5764, https://doi.org/10.3390/su14105764.
[6] M.M. Emamjomeh, H.A. Jamali, Z. Naghdali, M. Mousazadeh, Carwash wastewater treatment by the application of an environmentally friendly hybrid system: an experimental design approach, Desalin. WATER Treat. 160 (2019) 171–177, https://doi.org/10.5004/dwt.2019.24382.
[7] E. Kowsalya, S. Subashini, S. Sharmila, L.J. Rebecca, Treatment of carwash waste water and its reuse to manage water supply, Int. J. Recent Technol. Eng. 8 (2020) 3605–3610, https://doi.org/10.35940/ijrte.E6030.018520.
[8] G. Kashi, S. Younesi, A. Heidary, Z. Akbarishahabi, B. Kavianpour, R.R. Kalantary, Carwash wastewater treatment using the chemical processes, Water Sci. Technol. (2021), https://doi.org/10.2166/wst.2021.206.
[9] D. Dadebo, M. Nasr, M. Fujii, M.G. Ibrahim, Bio-coagulation using Cicer arietinum combined with pyrolyzed residual sludge-based adsorption for carwash wastewater treatment: a techno-economic and sustainable approach, J. Water Process Eng. 49 (2022) 103063, https://doi.org/10.1016/j.jwpe.2022.103063.
[10] I.M. Atiyah, B.A. Abdul-Majeed, Carwash wastewater treatment by electrocoagulation using aluminum foil electrodes, J. Eng. 25 (2019) 50–60, https://doi.org/10.31026/j.eng.2019.10.04.
[11] T. Hamada, Y. Miyazaki, Reuse of carwash water with a cellulose acetate ultrafiltration membrane aided by flocculation and activated carbon treatments, Desalination 169 (2004) 257–267, https://doi.org/10.1016/j.desal.2004.02.089.
[12] K. Boussu, G. Van Baelen, W. Colen, D. Eelen, S. Vanassche, C. Vandecasteele, B. Van der Bruggen, Technical and economical evaluation of water recycling in the carwash industry with membrane processes, Water Sci. Technol. 57 (2008) 1131–1135, https://doi.org/10.2166/wst.2008.236.
[13] M. Fedoryak, O. Boruk, S. Boruk, I. Winkler, Adsorption of the petrochemical pollutants released at the small vehicle-service facilities on the coal refinery sludge/pyrocarbon compositions, Inżynieria Miner. 1 (2021), https://doi.org/10.29227/IM-2021-01-08.
[14] S.-K. Hsu, C.-H. Chen, W.-K. Chang, Reclamation of car washing wastewater by a hybrid system combining bio-carriers and non-woven membranes filtration, Desalination Water Treat. 34 (2011) 349–353, https://doi.org/10.5004/dwt.2011.2046.
[15] X. Liu, Y. Shan, S. Zhang, Q. Kong, H. Pang, Application of metal organic framework in wastewater treatment, Green Energy Environ. (2023), https://doi.org/10.1016/j.gee.2022.03.005.
[16] M. Salehipour, S. Rezaei, H.F. Asadi Khalili, A. Motaharian, M. Mogharabi-Manzari, Nanoarchitectonics of enzyme/metal–organic framework composites for wastewater treatment, J. Inorg. Organomet. Polym. Mater. 32 (2022) 3321–3338, https://doi.org/10.1007/s10904-022-02390-1.
[17] V. Russo, M. Hmoudah, F. Broccoli, M.R. Iesce, O.-S. Jung, M. Di Serio, Applications of metal organic frameworks in wastewater treatment: a review on adsorption and photodegradation, Front. Chem. Eng. 2 (2020), https://doi.org/10.3389/fceng.2020.581487.
[18] H. Kaur, N. Devi, S.S. Siwal, W.F. Alsanie, M.K. Thakur, V.K. Thakur, Metal–organic framework-based materials for wastewater treatment: superior adsorbent materials for the removal of hazardous pollutants, ACS Omega 8 (2023) 9004–9030, https://doi.org/10.1021/acsomega.2c07719.
[19] W. Meng, S. Wang, H. Lv, Z. Wang, X. Han, Z. Zhou, J. Pu, Porous cellulose nanofiber (CNF)-based aerogel with the loading of zeolitic imidazolate frameworks-8 (ZIF-8) for Cu(II) removal from wastewater, Bioresources (2022), https://doi.org/10.15376/biores.17.2.2615-2631.
[20] Z. Pouramini, S.M. Mousavi, A. Babapoor, S.A. Hashemi, C.W. Lai, Y. Mazaheri, W.-H. Chiang, Effect of metal atom in zeolitic imidazolate frameworks (ZIF-8 & 67) for removal of dyes and antibiotics from wastewater: a review, Catalysts 13 (2023) 155, https://doi.org/10.3390/catal13010155.
[21] S. Denning, A.A.A. Majid, J.M. Lucero, J.M. Crawford, M.A. Carreon, C.A. Koh, Methane hydrate growth promoted by microporous zeolitic imidazolate frameworks ZIF-8 and ZIF-67 for enhanced methane storage, ACS Sustain. Chem. Eng. (2021), https://doi.org/10.1021/acssuschemeng.1c01488.
[22] M.R. Abdul Hamid, T.C. Shean Yaw, M.Z. Mohd Tohir, W.A. Wan Abdul Karim Ghani, P.D. Sutrisna, H.-K. Jeong, Zeolitic imidazolate framework membranes for gas separations: current state-of-the-art, challenges, and opportunities, J. Ind. Eng. Chem. 98 (2021) 17–41, https://doi.org/10.1016/j.jiec.2021.03.047.
[23] F. Naz, F. Mumtaz, S. Chaemchuen, F. Verpoort, Correction to: bulk ring-opening polymerization of ε-caprolactone by zeolitic imidazolate framework, Catal. Lett. 149 (2019) 2950–2951, https://doi.org/10.1007/s10562-019-02863-y.
[24] J.O. Ighalo, S. Rangabhashiyam, C.A. Adeyanju, S. Ogunniyi, A.G. Adeniyi, C. A. Igwegbe, Zeolitic Imidazolate Frameworks (ZIFs) for aqueous phase adsorption – a review, J. Ind. Eng. Chem. (2022), https://doi.org/10.1016/j.jiec.2021.09.029.
[25] H. Konno, S. Sasaki, Y. Nakasaka, T. Masuda, Facile synthesis of zeolitic imidazolate framework-8 (ZIF-8) particles immobilized on aramid microfibrils for wastewater treatment, Chem. Lett. 47 (2018) 620–623, https://doi.org/10.1246/cl.171215.
[26] S.Z.N. Ahmad, W.N.W. Salleh, N.H. Ismail, N.A.M. Razali, R. Hamdan, A.F. Ismail, Effects of operating parameters on cadmium removal for wastewater treatment using zeolitic imidazolate framework-L/graphene oxide composite, J. Environ. Chem. Eng. 9 (2021) 106139, https://doi.org/10.1016/j.jece.2021.106139.
[27] K. Li, N. Miwornunyuie, L. Chen, H. Jingyu, P.S. Amaniampong, D. Ato Koomson, D. Ewusi-Mensah, W. Xue, G. Li, H. Lu, Sustainable application of ZIF-8 for heavy-metal removal in aqueous solutions, Sustainability 13 (2021) 984, https://doi.org/10.3390/su13020984.
[28] Orooji, Emami Ghasali, Noorisafa, Razmjou, ANOVA design for the optimization of TiO2 coating on polyether sulfone membranes, Molecules 24 (2019) 2924, https://doi.org/10.3390/molecules24162924.
[29] A.S. Eltaweil, I.M. Mamdouh, E.M. Abd El-Monaem, G.M. El-Subruiti, Highly efficient removal for methylene blue and Cu2+onto UiO-66 metal-organic framework/carboxylated graphene oxide-incorporated sodium alginate beads, ACS Omega (2021), https://doi.org/10.1021/acsomega.1c03479.
[30] A.K.S. Jeevaraj, M. Muthuvinayagam, Graphene Oxide, Eng. Mater., 2023, pp. 91–104, https://doi.org/10.1007/978-981-99-1206-3_5.
[31] M. Hanbali, H. Holail, H. Hammud, Remediation of lead by pretreated red algae: adsorption isotherm, kinetic, column modeling and simulation studies, Green Chem. Lett. Rev. (2014), https://doi.org/10.1080/17518253.2014.955062.
[32] G. Yan, T. Viraraghavan, M. Chen, A new model for heavy metal removal in a biosorption column, Adsorpt. Sci. Technol. 19 (2001) 25–43, https://doi.org/10.1260/0263617011493953.
[33] R.M. Clark, Evaluating the cost and performance of field-scale granular activated carbon systems, Environ. Sci. Technol. 21 (1987) 573–580, https://doi.org/10.1021/es00160a008.
[34] Y.B. Utepov, A.K. Aldungarova, T. Mkilima, I.M. Pidal, A.S. Tulebekova, S. Z. Zharassov, A.K. Abisheva, Dynamics of embankment slope stability under combination of operating water levels and drawdown conditions, Infrastructure 7 (2022) 65, https://doi.org/10.3390/infrastructures7050065.
[35] K. Meiramkulova, D. Devrishov, Z. Adylbek, A. Kydyrbekova, S. Zhangazin, R. Ualiyeva, A. Temirbekova, G. Adilbektegi, T. Mkilima, The impact of various LED light spectra on tomato preservation, Sustainability 15 (2023) 1111, https://doi.org/10.3390/su15021111.
[36] R. Rai, S. Sharma, D.B. Gurung, B.K. Sitaula, R.D.T. Shah, Assessing the impacts of vehicle wash wastewater on surface water quality through physico-chemical and benthic macroinvertebrates analyses, Water Sci (2020), https://doi.org/10.1080/11104929.2020.1731136.
[37] J.C.P.S. Restrepo, D.I. Antonelo, T.S. Pokrywiecki, I.B. Tonial, F.C. Manosso, I.V. de Almeida, V.E.P. Vicentini, E. Düsman, Changes in physicochemical and toxicological parameters of waters of Trincheira's River caused by road construction, Ambient. e Agua - An Interdiscip. J. Appl. Sci. 14 (2019) 1, https://doi.org/10.4136/ambi-agua.2360.
[38] E.M. Anifah, I.K. Ariani, R.N. Hayati, S.A. Nugraha, Adsorption of oil and grease in wastewater using activated carbon derived from sewage sludge, IOP Conf. Ser. Earth Environ. Sci. (2022), https://doi.org/10.1088/1755-1315/1098/1/012043.
[39] I.R. Chowdhury, S. Chowdhury, M.A.J. Mazumder, A. Al-Ahmed, Removal of lead ions (Pb2+) from water and wastewater: a review on the low-cost adsorbents, Appl. Water Sci. 12 (2022) 185, https://doi.org/10.1007/s13201-022-01703-6.
[40] S. Moosavi, C.W. Lai, S. Gan, G. Zamiri, O. Akbarzadeh Pivehzhani, M.R. Johan, Application of efficient magnetic particles and activated carbon for dye removal from wastewater, ACS Omega 5 (2020) 20684–20697, https://doi.org/10.1021/acsomega.0c01905.
[41] M.D. Yahya, I.B. Muhammed, K.S. Obayomi, A.G. Olugbenga, U.B. Abdullahi, Optimization of fixed bed column process for removal of Fe(II) and Pb(II) ions from thermal power plant effluent using NaoH-rice husk ash and Spirogyra, Sci. African. 10 (2020) e00649, https://doi.org/10.1016/j.sciaf.2020.e00649.
[42] I. Kamal, F. Albadran, H. Jaafar, D. Ali, M. Alfaize, Continuous flow adsorption for phenol removal using environmentally friendly naturally derived bed, IOP Conf. Ser. Mater. Sci. Eng. (2020), https://doi.org/10.1088/1757-899X/928/2/022050.
[43] G. El Mouhri, M. Merzouki, H. Belhassan, Y. Miyah, H. Amakdouf, R. Elmountassir, A. Lahrichi, Continuous adsorption modeling and fixed bed column studies: adsorption of tannery wastewater pollutants using beach sand, J. Chem. 2020 (2020) 1–9, https://doi.org/10.1155/2020/7613484.
[44] I.N. Shaikh, M.M. Ahammed, Granular media filtration for on-site treatment of greywater: a review, Water Sci. Technol. 86 (2022) 992–1016, https://doi.org/10.2166/wst.2022.269.
[45] K. Meiramkulova, T. Mkilima, G. Baituk, K. Beisembayeva, A. Meirbekov, A. Kakabayev, G. Adilbektegi, A. Tleukulov, G. Tazhkenova, Treatment of waste stabilization pond effluent using natural zeolite for irrigation potential, PLoS One 17 (2022) e0259614, https://doi.org/10.1371/journal.pone.0259614.